Proc. Natl. Acad. Sci. USA
Vol. 96, pp. 3513–3518, March 1999
Applied Biological Sciences

A cytosine analog that confers enhanced potency to antisense oligonucleotides

W. MICHAEL FLANAGAN*†, JOHN J. WOLF, PETER OLSON, DEBBIE GRANT, KUEI-YING LIN, RICHARD W. WAGNER‡, AND MARK D. MATTEUCCI*

Gilead Sciences, 333 Lakeside Drive, Foster City, CA 94404

Communicated by Marvin H. Caruthers, University of Colorado, Bouder, CO, February 1, 1999 (received for review October 6, 1998)

ABSTRACT **Antisense technology is based on the ability to design potent, sequence-specific inhibitors. The G-clamp heterocycle modification, a cytosine analog that clamps on to guanine by forming an additional hydrogen bond, was rationally designed to enhance oligonucleotide/RNA hybrid affinity. A single, context-dependent substitution of a G-clamp heterocycle into a 15-mer phosphorothioate oligodeoxynucleotide (S-ON) targeting the cyclin-dependent kinase inhibitor, $p27^{kip1}$, enhanced antisense activity as compared with a previously optimized C5-propynyl-modified $p27^{kip1}$ S-ON and functionally replaced 11 C5-propynyl modifications. Dose-dependent, sequence-specific antisense inhibition was observed at nanomolar concentrations of the G-clamp S-ONs. A single nucleotide mismatch between the G-clamp S-ON and the $p27^{kip1}$ mRNA reduced the potency of the antisense ON by five-fold. A 2-base-mismatch S-ON eliminated antisense activity, confirming the sequence specificity of G-clamp-modified S-ONs. The G-clamp-substituted $p27^{kip1}$ S-ON activated RNase H-mediated cleavage and demonstrated increased *in vitro* binding affinity for its RNA target compared with conventional 15-mer S-ONs. Furthermore, incorporation of a single G-clamp modification into a previously optimized 20-mer phosphorothioate antisense S-ON targeting c-raf increased the potency of the S-ON 25-fold. The G-clamp heterocycle is a potent, mismatch-sensitive, automated synthesizer-compatible antisense S-ON modification that will have important applications in the elucidation of gene function, the validation of gene targets, and the development of more potent antisense-based pharmaceuticals.**

Several methods have been developed to validate drug targets and provide insight at the molecular level of diseases. These methods include targeted deletions in mice, antibodies, aptamers, ribozymes, and antisense oligodeoxynucleotides (ONs). Effective antisense ONs have the additional option of being developed into human therapeutics.

Antisense ONs are short (7–30 nt), synthetic pieces of DNA that are rationally designed to selectively hybridize to a target RNA and interfere with the expression of the encoded protein. An effective antisense ON inhibitor must be stable to omnipresent nucleases and demonstrate high affinity for its target RNA sequence. An effective inhibitor, in most cases, is recognized by intracellular RNase H on binding to its RNA target, and the RNA portion is degraded (1).

The first ONs tested in tissue culture were phosphodiester ONs (2). They were rapidly degraded by nucleases in culture media and, thus, showed poor antisense activity (3, 4). The phosphorothioate internucleotide linkage has circumvented this problem and has emerged as the analog of choice for creating nuclease-resistant ONs. One drawback of phosphorothioate-modified ONs is that they have decreased binding affinity for their RNA target compared with their phosphodiester-containing predecessors.

To enhance the binding affinity of phosphorothioate ONs, many ON modifications have been synthesized and tested for more potent antisense activity (reviewed in ref. 5). Identifying potent ONs is critical in developing antisense-based human therapeutics, because more potent ONs will allow for lower doses to be used. This will reduce the overall cost of therapy and alleviate the ON-related toxicities that have been observed in the clinic (reviewed in ref. 6).

Recently, we described a cytosine analog, termed G-clamp, that forms an additional hydrogen bond to guanine (7) (Fig. 1). The G-clamp base modification recognizes both the Watson–Crick and Hoogsteen faces of the complementary guanine within a helix. Binding studies demonstrated that a single G-clamp substitution within an antisense ON dramatically enhanced helical thermal stability and mismatch discrimination. However, the bioactivity of G-clamp-modified antisense ONs was unknown. For this report, we examined the sequence-context dependence, antisense activity, mismatch sensitivity, RNAse H cleavage, and hybridization kinetics of a 15-mer $p27^{kip1}$ phosphorothioate oligodeoxynucleotide (S-ON) containing single G-clamp substitutions. The data demonstrate that a single G-clamp substitution in a 15-mer S-ON conferred mismatch sensitivity and enhanced potency to the antisense S-ON as compared with our previous most potent multiply substituted C5-propynyl-modified S-ON. Furthermore, incorporation of a G-clamp into a previously optimized 20-mer S-ON targeting c-*raf* also dramatically increased the potency of the S-ON. These data demonstrate that the G-clamp modification is a highly potent, portable, and mismatch-sensitive cytosine analog.

MATERIALS AND METHODS

Cell Culture. African green monkey kidney cells (CV-1 cells, American Type Culture Collection) were maintained in DMEM supplemented with 10% fetal calf serum. The T24 bladder carcinoma cell line was purchased from American Type Culture Collection and were cultured according to the recommended conditions.

S-ON Synthesis, Purification, and Sequences. S-ONs were synthesized by the H-phosphonate method on an automated synthesizer (model 8750, MilliGen/Biosearch) by using standard chemistry on controlled pore glass support (8). The nucleoside analogs were prepared as described (7, 9, 10). Sequences of the c-*raf* S-ONs are GS4204 (the same as ISIS 5132) 5′-TCC CGC CTG TGA CAT GCA TT (11), GS4206 (a

The publication costs of this article were defrayed in part by page charge payment. This article must therefore be hereby marked "*advertisement*" in accordance with 18 U.S.C. §1734 solely to indicate this fact.

PNAS is available online at www.pnas.org.

Abbreviations: ON, oligodeoxynucleotide; S-ON, phosphorothioate-ON; PI3K, phosphoinositide 3-kinase.

*To whom reprint requests should be addressed. e-mail: mflanagan@sunesis-pharma.com or mark_matteucci@gilead.com.

†Present address: Sunesis Pharmaceuticals, 3696 Haven Avenue, Suite C, Redwood City, CA 94063.

‡Present address: Phylos, Inc., 128 Spring Street, Lexington, MA 02421.

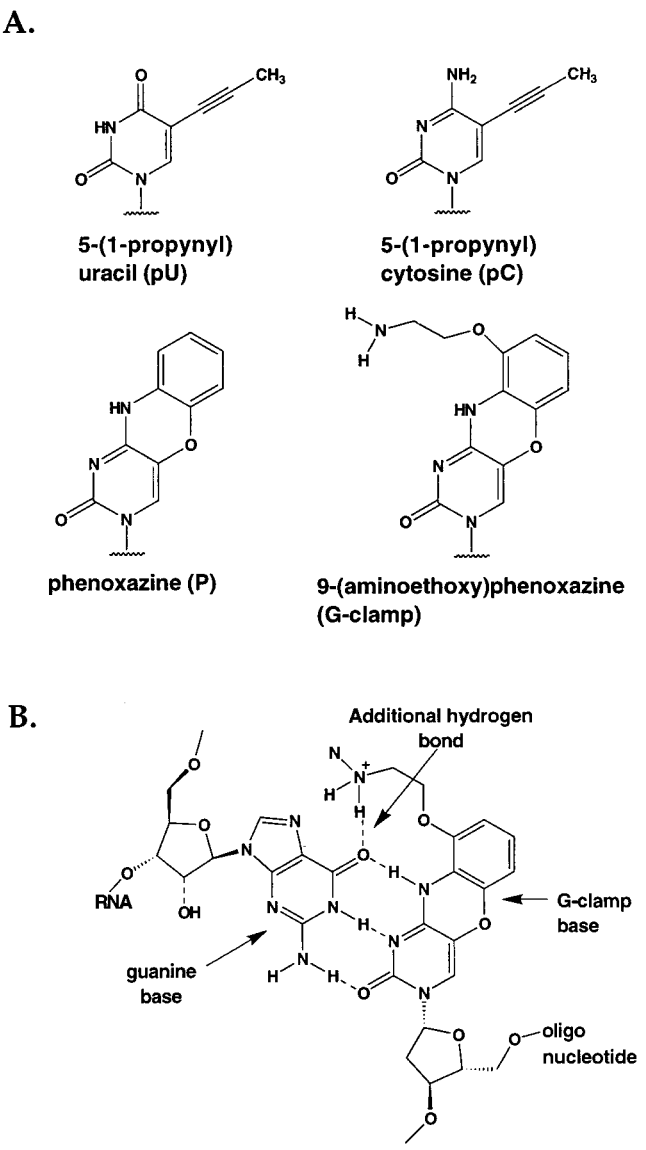

FIG. 1. (*A*) Chemical structure of heterocycle analogs. (*B*) Model of G-clamp hybridized to guanine within a RNA/oligonucleotide helix.

4-nt mismatch; *italics* denote the mismatch sites) 5′-TCC CGC CT*A CTT* CAT GCA TT, GS5628 (the G-clamp-modified equivalent to ISIS 5132; X indicates the G-clamp heterocycle) 5′-TCX CGC CTG TGA CAT GCA TT, and GS6206 (the G-clamp mismatch to GS5628, X indicates the G-clamp heterocycle and *italics* denote the mismatch sites) 5′-TC*G* C*X*C CTG *AGT* CAT GCA TT. C denotes 2′-deoxycytidine only in the c-*raf* series and 2′-deoxy-5-methylcytidine in the $p27^{kip1}$ series.

Hybridization and Dissociation Rates of S-ON/RNA Complexes. The relative kinetics of hybridization and dissociation of S-ON/RNA complexes *in vitro* was performed as described by using ^{32}P-labeled RNA complementary to the $p27^{kip1}$ antisense S-ONs (12, 13). The amount of probe hybridized to the antisense S-ON at each time point was quantitated by using a Storm 860 PhosphorImager (Molecular Dynamics).

RNase H Cleavage Assay. The RNase H cleavage assay was performed as described (12, 13). Briefly, [^{32}P]RNA was bound to 5 nM ON for 1 h in RNase H buffer [50 mM Tris·Cl, pH 8.0/10 mM $MgCl_2$/20 mM KCl/3 mM DTT/40 units of RNasin (Promega)]. HeLa nuclear extract (100 ng; Promega) was added for various times; the reactions were frozen on dry ice and, subsequently, electrophoresed on a 20% PAGE containing 8.3 M urea. For base hydrolysis controls, RNA was added to a 4 mM NaOH solution and heated to 95°C for 5 min. Gels were quantitated by using a Storm 860 PhosphorImager (Molecular Dynamics). Percent cleavage refers to the relative amount of the S-ON/RNA duplex that degraded as a result of RNase H cleavage.

Microinjection Assay. Microinjection, immunofluorescence staining, and fluorescence microscopy were carried out as described (14–17).

Cytofectin Reagent. GS3815 cytofectin (Glen Research, Sterling, VA) is a formulation of two equivalents of a cationic lipid (dimyristylamidoglycyl-*N*-α-isopropoxycarbonyl-arginine dihydrochloride, GS3815) with one equivalent of the zwitterion L-α-dioleoylphosphatidylethanolamine (DOPE, Avanti Polar Lipids). GS3815 cytofectin is a replacement of GS2888 cytofectin because it has long-term stability at both 4°C and −20°C (ref. 18). The only difference between GS3815 and GS2888 is the replacement of the *t*-butyloxycarbonyl group of GS2888 with isopropyloxycarbonyl. GS3815 cytofectin delivers S-ONs and plasmid DNA efficiently to a broad spectrum of cell lines in the presence of serum-containing growth media with little or no cytotoxicity.

Oligonucleotide Delivery. Delivery of S-ONs to cells was carried out as described (18–22). Briefly, cells were grown in 100-mm tissue culture plates to a cell density of 60–80% cell confluence on the day of the transfection. The S-ON was diluted into 200 μl of prewarmed OptiMEM (GIBCO/BRL) in a polystryrene plate and mixed with 200 μl of prewarmed OptiMEM containing GS3815 cytofectin. The mixture (400 μl) was incubated at room temperature for 10–15 min. Complete growth media (3.6 ml) was added to the S-ON/lipid mixture. The media from the cells was removed and replaced with the 4 ml of the S-ON/lipid transfection mixture. Final concentration of the S-ON in the 4 ml of media varied between 1 and 90 nM depending on the experiment. The GS3815 cytofectin was used at a final concentration of 2.5 μg/ml. The transfection mixture was incubated with the cells for 4–6 h, and an additional 4 ml of complete growth media was added to the S-ON/lipid transfection mixture incubating on top of the cells. The S-ON/cytofectin complex was left on the cells for 24–48 h before preparing protein extracts.

Plasmids. The wild-type human $p27^{kip1}$ plasmid was previously described (19). The mutant $p27^{kip1}$ plasmid containing a thymidine substitution for the guanine at position 312 (GenBank accession no. U10906) was constructed by using primers and PCR to create a 1-bp mismatch as described (19) and was confirmed by sequencing. The sequence of the wild-type $p27^{kip1}$ at this site is 5′-GGC GCA GGA GAG CCA (human sequences 306–320). The $p27^{kip1}$ mutant sequence 5′-GGC GCA *T*GA GAG CCA (the *italicized* nucleotide denotes the mismatch base at 312).

Immunoblot Analysis. Cellular extracts were prepared as described (16, 20, 21). Electrophoretic and transfer conditions have been described (16, 20, 21). The $p27^{kip1}$ mAb was used at a 1:1,000 dilution (Transduction Laboratories, Lexington, KY), and phosphoinositide 3-kinase (PI3K) p85 subunit polyclonal antibody was used at 1:10,000 dilution (Upstate Biotechnology Inc, Lake Placid, NY). Blots were developed by using horseradish peroxidase-conjugated goat anti-rabbit and/or anti-mouse antibodies (1:5,000 or 1:1,000, respectively; Zymed) and the enhanced chemiluminescence (ECL) Western blotting detection reagents (as per instructions, Amersham Pharmacia). Membranes were exposed to X-Omat AR film (Eastman Kodak). The immunoblots were quantitated by using a Storm 860 PhosphorImager (Molecular Dynamics) and ECL^+ Western blotting detection reagents (Amersham Pharmacia) or by densitometry. All samples were normalized to PI3K or p34cdc2 to control for variations in protein loading or transfer to the immunoblot membrane.

RESULTS

The Potency of the G-Clamp Modification Is Context-Dependent. The G-clamp modification was singly substituted at every possible cytosine within the $p27^{kip1}$ S-ON and tested for antisense activity (Fig. 2*A*). The antisense ON/cytofectin mixture was incubated with CV-1 cells for 24 h, and protein extracts were then prepared from the cells, immunoblotted, and analyzed for $p27^{kip1}$ protein levels. As shown in Fig. 2*B*, the bioactivity of the G-clamp-modified $p27^{kip1}$ S-ONs depended on the sequence context. Results from six of the seven G-clamp-modified $p27^{kip1}$ S-ONs are shown. G-clamp modification of the 3′ cytosine (ON7) demonstrated poor antisense activity at 30 nM (data not shown). Comparison of the antisense activity of the six G-clamp-modified S-ONs demonstrated that ON4 was the most potent. At 10 nM, ON4 inhibited $p27^{kip1}$ protein levels by 84% compared with the GS3815 cytofectin-only control (Fig. 2*B*, lanes 1 and 10). The rank-order potency of the six G-clamp S-ONs was ON4 > ON6 > ON3 = ON2 > ON5 > ON1. Similar rank-order potency of the S-ONs was obtained when the G-clamp S-ONs were tested by microinjection into the nuclei of CV-1 cells (data not shown). These results indicate that the antisense activity of the S-ONs depended on the sequence context of the G-clamp modification rather than variations in S-ON delivery to CV-1 cells by using GS3815 cytofectin.

G-Clamp Modified Phosphorothioate ONs Are Potent Antisense Inhibitors. The antisense activity of the most potent G-clamp modified S-ON targeting $p27^{kip1}$ (ON4) was evaluated and compared with the 5-methylcytosine control, a phenoxazine-modified, and a multiply substituted C5-propynyl-modified sequence after transfection of the individual antisense S-ONs into CV-1 cells. Structures of the base analogs are shown in Fig. 1 (see Table 2 for sequences). Dose-dependent antisense activity was seen for the C5-propynyl, phenoxazine-, and G-clamp-modified $p27^{kip1}$ S-ONs (Fig. 3, lanes 2–4 and 8–13). The control S-ON failed to demonstrate any antisense activity under the conditions tested (Fig. 3, lanes 5–7). At 30 nM, the G-clamp antisense S-ON inhibited $p27^{kip1}$ expression by 96% as compared with the lipid control (Fig. 3, compare lane 1 to 13), consistent with results shown in Fig. 2*B*. The IC_{50} for the G-clamp $p27^{kip1}$ S-ON is between 3 and 5 nM (Fig. 3, compare lanes 11–13 with lane 1). The phenoxazine S-ON, the tricyclic core of the G-clamp, decreased $p27^{kip1}$ levels by 79% at 30 nM, whereas 30 nM of our most potent C5 propynyl $p27^{kip1}$ S-ON, which has 11 C5-propynyl-modified bases, decreased $p27^{kip1}$ levels by 67% consistent with previous results (19, 22). Comparison of the antisense activities of S-ONs indicated that the G-clamp S-ON is 3-fold more potent than the multiply substituted C5-propynyl S-ON targeting $p27^{kip1}$ (Fig. 3, compare $p27^{kip1}$ levels in lanes 4 and 12). These data demonstrate that a single G-clamp modification can functionally replace 11 C5 propyne modifications in the 15-mer S-ON targeting $p27^{kip1}$ and confers enhanced antisense potency.

G-Clamp S-ONs Are Sequence-Selective Inhibitors. To demonstrate that the inhibition of $p27^{kip1}$ by G-clamp S-ONs was a sequence-specific antisense effect, a 2-nt mismatch G-clamp S-ON was synthesized, transfected into CV-1 cells using GS3815 cytofectin, and analyzed for its effect on $p27^{kip1}$ expression. The 2-nt mismatch S-ON was constructed by switching the G-clamp base with a nearby thymidine base (5′-TGG CTC *XCT* TGC GCC; X indicates the position of the G-clamp modification and *italics* indicates mismatch positions). The overall base composition of the G-clamp antisense and mismatch S-ONs was identical. The 2-nt mismatch S-ON, when normalized to the internal PI3K control, had no effect on $p27^{kip1}$ expression at 90 nM, an S-ON concentration that is 20- to 30-fold higher than the IC_{50} for the perfectly matched S-ON. The $p27^{kip1}$ antisense G-clamp S-ON demonstrated nearly complete inhibition of $p27^{kip1}$ even when titrated from 90 to 10 nM (Fig. 4, lanes 3–5). These data indicate that the G-clamp S-ON-mediated inhibition of $p27^{kip1}$ is due to a sequence-dependent antisense mechanism of action.

To rigorously test the sequence specificity of the G-clamp-modified S-ON, the antisense binding site in the $p27^{kip1}$ expression vector was mutated at a single base pair and microinjected with the G-clamp S-ON that targeted wild-type $p27^{kip1}$ (ON4). The mutation in the $p27^{kip1}$ expression vector changed the complementary guanosine in the transcribed mRNA, which hybridized to the G-clamp modification, to a uracil. Although the G-to-U substitution resulted in an amino

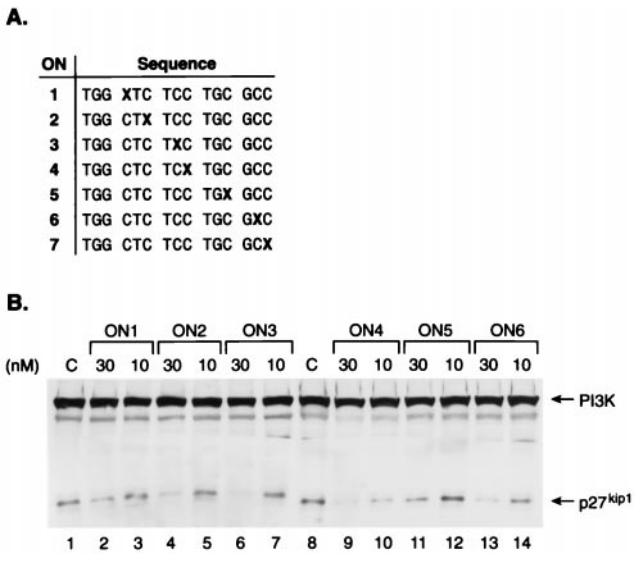

FIG. 2. The bioactivity of the G-clamp-modified $p27^{kip1}$ S-ON is context-dependent. (*A*) Sequence and position of the G-clamp modification (G-clamp is denoted by **X**) tested for $p27^{kip1}$ antisense activity. All linkages are phosphorothioate. T, thymidine; G, 2′-deoxyguanosine; C, 2′-deoxy-5-methylcytidine. (*B*) Immunodetection of $p27^{kip1}$ and PI3K (p85 regulatory subunit) after transfection of CV-1 cells with GS3815 cytofectin alone (2.5 μg/ml; lane 1), or GS3815 cytofectin (2.5 μg/ml) complexed with 30 or 10 nM of ON1 (lanes 2 and 3), ON2 (lanes 4 and 5), ON3 (lanes 6 and 7), ON4 (lanes 9 and 10), ON5 (lanes 11 and 12), or ON6 (lanes 13 and 14). At 30 nM, ON1 inhibited $p27^{kip1}$ protein levels by 40%, ON2 by 72%, ON3 by 88%, ON4 by 98%, ON5 by 54%, and ON6 by 98%. No inhibition of $p27^{kip1}$ protein levels was observed for ON1, ON2, ON3, and ON5 at 10 nM. The two most potent S-ONs, ON4 and ON6, inhibited $p27^{kip1}$ protein levels by 84 and 57%, respectively, at 10 nM (lanes 10 and 14). PI3K was used as an internal control for protein integrity, concentration, and transfer variations among the samples.

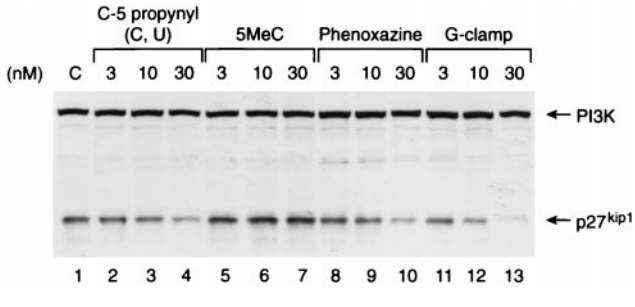

FIG. 3. The G-clamp-modified $p27^{kip1}$ S-ON demonstrates potent, dose-dependent antisense inhibition. Immunodetection of $p27^{kip1}$ and PI3K (p85 regulatory subunit) after transfection of CV-1 cells with GS3815 cytofectin (lane 1); C5-propynyl with 11 substitutions (ON8; lanes 2–4)(see Table 2 for sequences); 5MeC, 5-methylcytosine control (ON9; lanes 5–7); phenoxazine-modified (ON10; lanes 8–10), and G-clamp modified (ON4; lanes 11–13) using 2.5 μg/ml GS3815 cytofectin and a range of S-ON concentrations (30, 10, and 3 nM).

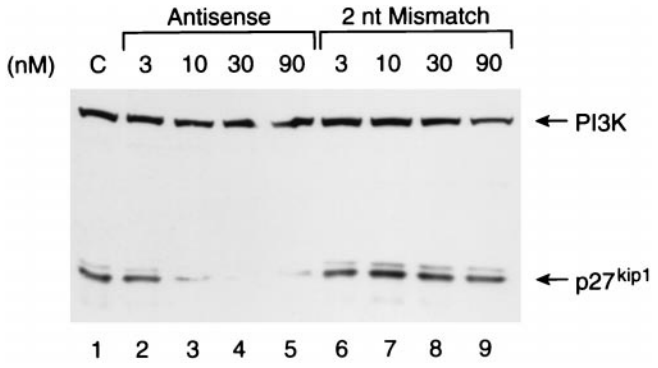

FIG. 4. G-clamp-modified S-ONs demonstrate sequence-specific inhibition of $p27^{kip1}$. Immunoblot analysis of PI3K and $p27^{kip1}$ in CV-1 cells transfected with 2.5 μg/ml GS3815 cytofectin complexed in the absence (lane 1) or presence of a range of concentrations of the G-clamp-modified S-ON, ON4, (lanes 2–5), or 2-nt-mismatch G-clamp-modified S-ONs (lanes 6–9). The sequence for the 2-nt G-clamp $p27^{kip1}$ mismatch S-ON is 5′-TGG CTC *XCT* TGC GCC, where the X indicates the position of the G-clamp substitution and italics denotes the mismatch sites. The G-clamp-modified $p27^{kip1}$ antisense S-ON inhibited $p27^{kip1}$ by 98.8% at 90 nM, 95.4% at 30 nM, 81.0% at 10 nM, and 26.7% at 3 nM when normalized to PI3K and compared with $p27^{kip1}$ protein levels in the control lane (lane 1, GS3815 cytofectin only). No effects on $p27^{kip1}$ levels were seen in extracts treated with the 2-nt mismatch S-ON. At 90, 30, 10, and 3 nM of the mismatch S-ON, $p27^{kip1}$ was expressed at 112, 107, 119, and 100%, respectively, of the control lane.

acid change in $p27^{kip1}$, expression of the mutant $p27^{kip1}$ was unaffected as compared with the wild-type $p27^{kip1}$ expression after microinjection (data not shown). The mutant or the wild-type p27 plasmid was microinjected with the G-clamp S-ON-targeting $p27^{kip1}$. A plasmid that expressed β-galactosidase was coinjected as an internal control and marker for injected cells. Eighteen hours later, the cells were fixed, immunostained, and the β-galactosidase-positive cells were analyzed for $p27^{kip1}$ expression. Microinjection of the two $p27^{kip1}$ plasmids with the C5-propynyl-modified $p27^{kip1}$ antisense S-ON was also done for comparison. Both modified $p27^{kip1}$ S-ONs inhibited expression of the wild-type $p27^{kip1}$ plasmid (Table 1), consistent with the transfection results shown in Fig. 3. No effect on β-galactosidase expression was observed. A 5-fold reduction in antisense activity was observed for the G-clamp S-ON when targeting the mutant $p27^{kip1}$ (Table 1, ON4, compare IC_{50} of 0.05 to 0.25 μM). In contrast, the bioactivity of the C5-propynyl S-ON was essentially unaffected by a single mismatch in the $p27^{kip1}$ target sequence. IC_{50} for wild-type $p27^{kip1}$ was 0.20 μM, whereas the IC_{50} for the mutated plasmid was 0.25 μM. These results confirm that the G-clamp $p27^{kip1}$ S-ON functions by an antisense mechanism of action and further demonstrate that the G-clamp S-ON is a potent, sequence-specific, and target-selective antisense inhibitor.

Table 1. Single-nucleotide mismatch selectivity of base-modified S-ONs

ON	Sequence	Base modifications	$p27^{kip1}$ IC_{50}, μM	
			Wild-type	Mutant
8	**UGG CUC UCC UGC GCC**	pC, pU	0.20	0.25
4	TGG CTC TC**X** TGC GCC	G-clamp	0.05	0.25

Boldface indicates the position of the substituted heterocycle modification. S-ON modifications are shown in Fig. 1. The ON 8 contains C5-propynyl (pC, pU) in the bold positions and in 4, X = G-clamp. All linkages are phosphorothioate. T, thymidine; G, 2′-deoxyguanosine; C, 2′-deoxy-5′-methylcytidine. IC_{50} values were determined by microinjection as described (15, 16, 17). Each experiment was repeated in triplicate. The wild-type and mutant $p27^{kip1}$ sequences differed by a single nucleotide. The guanine base at position 312 based on the human sequence (GenBank accession no. U10906) was changed to a thymidine. Sequences are: G-clamp S-ON, 3′-CCG CGT **X**CT CTC GGT; $p27^{kip1}$ wild-type RNA, 5′-GGC GCA GGA GAG CCA (human sequences 306–320); $p27^{kip1}$ mutant RNA, 5′-GGC GCA *U*GA GAG CCA (*italicized* nucleotide denotes the mismatch).

Hybridization Properties of G-Clamp-Modified S-ONs. A gel-shift assay (see *Materials and Methods*) was used to investigate the rates of association and dissociation of the four modified $p27^{kip1}$ S-ONs (G-clamp, unmodified, phenoxazine, and the multiply substituted C5-propynyl S-ONs) previously characterized for antisense potency in cell culture. As shown in Table 2, the G-clamp S-ON bound to its RNA target 1.7-fold faster than the unmodified S-ON and 1.9-fold faster than the phenoxazine S-ON; in contrast, the G-clamp bound 1.5-fold slower relative to the multiply substituted C5-propynyl S-ON.

Analysis of the dissociation rates of all of the modified S-ONs indicated no dramatic difference. The unmodified S-ON/RNA duplex, which showed the most rapid dissociation, showed 47% dissociation after 27 h, whereas the C5-propynyl S-ON and the G-clamp S-ON/RNA complexes were dissociated 28% and 36%, respectively. The relative rates of dissociation are 1.0 for the unmodified S-ON/RNA duplex, 0.77 for the G clamp, and 0.60 for the C5-propynyl S-ON.

Overall the G-clamp-modified S-ON has a relative affinity for its RNA target that is 2.2-fold greater than the unmodified S-ON and 2.7-fold greater than the phenoxazine S-ON. These modest effects correlate with the increased potency observed for the G-clamp S-ON as shown in Fig. 3. However, the multiply substituted C5-propynyl S-ON had the highest affinity, yet the G-clamp S-ON demonstrated the most potent antisense inhibition of $p27^{kip1}$.

G-Clamp S-ON Are RNase H-Competent. The lack of correlation between the affinity of the G-clamp S-ON and its enhanced antisense activity relative to the C5-propynyl S-ON suggested that the rate of RNase H cleavage of the target RNA may account for the increased potency of the G-clamp $p27^{kip1}$ antisense S-ON. To directly test this possibility, the same four modified S-ONs as above were tested and compared in their ability to activate RNase H cleavage of the target RNA. The S-ON/[^{32}P]RNA heteroduplexes were incubated with HeLa nuclear extracts (a source of human RNase H) for various times, and the cleavage products were analyzed. Reaction times were adjusted so that >70% of the S-ON/RNA heteroduplex was intact after RNase H cleavage. These conditions allow fine mapping of the cleavage site. The results indicate that the RNA portion of the G-clamp S-ON/RNA heteroduplex was efficiently cleaved by RNase H. No differences in the cleavage pattern were observed for the unmodified S-ON and the G-clamp S-ON (Table 2, ON10 and ON4, respectively), suggesting the single G-clamp modification in the major groove of the helix was easily accommodated by RNase H.

Analysis of the percent cleavage showed that the G-clamp S-ON/RNA duplex was cleaved 3.5-fold more rapidly than the C5-propynyl S-ON/RNA duplex (Table 2, compare ON4 and ON8). This difference in RNase H cleavage rate may, in part, account for the increased potency observed for the $p27^{kip1}$ G-clamp S-ON as compared with our previous most potent C5-propynyl $p27^{kip1}$ S-ON.

A Single G-Clamp Modification Enhanced the Potency of a Previously Optimized Antisense S-ON. To highlight the portability and potency of the G-clamp modification, a single G-clamp substitution was incorporated into a previously optimized antisense S-ON targeting c-*raf* (5′-TCX CGC CTG TGA CAT GCA TT; X = G-clamp) and tested for antisense activity. The first-generation c-*raf* antisense S-ON (5′-TCC CGC CTG TGA CAT GCA TT) was identified by Monia *et al.* (11, 23) as the most potent S-ON out of a screen of 34 distinct S-ONs spanning the entire c-*raf* gene. This 20-mer c-*raf* antisense S-ON is currently being tested in phase II trials for the treatment of cancer (reviewed in ref. 6).

Table 2. Biophysical properties and RNase H activity of S-ONs

ON	Sequence	Base modifications	k_{rel} on*	k_{rel} off*	K_{rel}†	RNase H, cleavage %‡
9	TGG CTC TCC TGC GCC	none	1.0	1.0	1	21.7
8	**U**GG **CUC UCCUGCGCC**	pC, pU	2.5	0.60	4.2	4.9
10	TGG CTC TC**P** TGC GCC	P	0.9	1.1	0.81	9.1
4	TGG CTC TC**X** TGC GCC	G-clamp	1.7	0.77	2.2	17.4

Boldface indicates the position of the substituted heterocycle modification. All eleven pyrimidines in ON8 are C5-propynyl-modified. S-ON base modifications are shown in Fig. 1. The S-ONs contain C5-propynyl (pC, pU), phenoxazine (P) and G-clamp (X). All linkages are phosphorothioate. T, thymidine; G, 2′-deoxyguanosine; C, 2′-deoxy-5′-methylcytidine.

*The relative association rates (k_{rel} on and k_{rel} off) were determined as described in *Materials and Methods*. The relative rates have been normalized to the value for the unmodified S-ON (ON9). For k_{rel} on, a value >1 indicates that the S-ON associates faster than the unmodified S-ON control. For k_{rel} off, a value <1 indicates that the S-ON dissociates slower than the unmodified S-ON control. Each of the above experiments were repeated in duplicate, and similar results were obtained.

†$K_{rel} = k_{rel}$ on/k_{rel} off.

‡The percent RNA cleavage by RNase H in HeLa nuclear extracts after 5 min at 37°C.

The antisense S-ONs and their corresponding 4-nt mismatch S-ONs were delivered to T24 bladder carcinoma cells by using 2.5 μg/ml GS3815 cytofectin and a range of S-ON concentrations. Based on earlier results (Fig. 3), the G-clamp S-ONs were tested at S-ON concentrations 10-fold lower than the unmodified S-ONs. Forty-eight hours later, protein extracts were prepared, separated by using SDS/PAGE, and analyzed for c-*raf* protein levels. The cyclin-dependent kinase (cdc2) was used as an internal control.

An antisense-specific decrease in c-*raf* levels was observed for both the G-clamp S-ON and the unmodified S-ON (Fig. 5) under all conditions tested. At 10 nM, the G-clamp c-*raf* S-ON specifically reduced c-*raf* protein levels by 63%,whereas the 4-nt G-clamp mismatch had no effect on c-*raf* levels. A similar 62% decrease in c-*raf* levels (Fig. 5, lane 2) was observed with the unmodified c-*raf* S-ON at a 25-fold higher S-ON concentration (250 nM) relative to the singly substituted G-clamp S-ON. These antisense results with the unmodified c-*raf* S-ONs are consistent with previous reports (11, 24). Our data suggest that incorporation of a single G-clamp modification, even into a previously optimized antisense S-ON, can dramatically enhance the potency of an antisense S-ON.

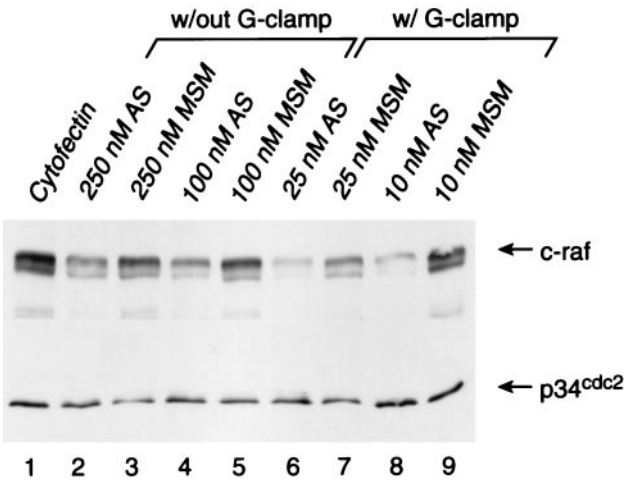

FIG. 5. Incorporation of a single G-clamp into an optimized c-*raf* antisense S-ON dramatically enhanced its antisense potency. T24 bladder carcinoma cells were transfected with GS3815 cytofectin (2.5 μg/ml) complexed with varying concentrations of an unmodified c-*raf* antisense (AS) S-ON; an unmodified 4-nt mismatch (MSM) S-ON; a G-clamp c-*raf* antisense (AS) S-ON; and a 4-nt G-clamp mismatch (MSM) S-ON. Note that the G-clamp modified c-*raf* S-ONs were tested at a 10-fold lower S-ON concentration than the unmodified c-*raf* S-ON. Forty-eight hours later, extracts were prepared and analyzed for c-*raf* levels by immunodetection. p34cdc2 was used as an internal control. At 250 nM (lane 2) and 100 nM (lane 4), the unmodified c-*raf* antisense S-ON demonstrated a reduction in c-*raf* protein levels of 62 and 29%, respectively, when normalized to p34cdc2 and compared with control c-*raf* levels (GS3815 cytofectin only, lane1). The unmodified 4-nt mismatch S-ON had no effect on c-*raf* protein levels (lanes 3 and 5). At 25 nM (lane 6) and 10 nM (lane 8), the G-clamp-modified c-*raf* antisense S-ON inhibited c-*raf* protein levels by 76 and 63%, respectively. The G-clamp-modified 4-nt mismatch S-ON showed a modest 20% decrease in c-*raf* protein levels at 25 nM of the S-ON (lane 7). No effect on c-*raf* protein levels was seen at 10 nM of the G-clamp modified 4-nt mismatch S-ON (lane 9).

DISCUSSION

The G-clamp modification is a remarkably potent heterocycle modification. A single G-clamp enhanced the potency of a S-ON relative to 11 C5-propynyl modifications yet retains the sequence selectivity of an unmodified base. For most S-ON modifications, there is a tradeoff between increased potency and sequence selectivity. For example, the fully C5-propynyl-modified $p27^{kip1}$ is a potent antisense inhibitor (Fig. 3) and shows high-affinity for its RNA target, yet it is insensitive to a single nucleotide mismatch, as shown in Table 1. The G-clamp $p27^{kip1}$ S-ON also is a potent inhibitor of $p27^{kip1}$, more potent than the C5-propynyl $p27^{kip1}$ S-ON, and, yet, it demonstrated a 5-fold reduction in antisense activity when a single nucleotide mismatch existed between the G-clamp modified $p27^{kip1}$ S-ON and its RNA target. A similar 5-fold reduction in activity was observed previously by using an unmodified 17-nt S-ON that selectively targeted a mutant *ras* gene containing a single base change at codon 12 (25). The sequence selectivity of the G-clamp $p27^{kip1}$ S-ON might be further increased by optimizing the length of the S-ON.

We have found that the position the G-clamp modification within the S-ON greatly influenced the antisense potency of the G-clamp substitution. As shown in Fig. 2, the antisense activity of the singly G-clamp-substituted $p27^{kip1}$ S-ONs varied after transfection into CV-1 cells. The reasons for this contextual or positional effect are at present unclear. Full elucidation of these effects will require further study. Until then, based on the limited data set, the tentative empirical conclusion is that the optimal position for a single G-clamp modification is between two pyrimidines.

In vitro analysis of several modified S-ONs indicated that the G-clamp S-ON hybridized faster and formed a more stable interaction relative to the unmodified S-ON or the phenoxazine S-ON, but the differences were small. This enhanced binding affinity translated into the increased potency observed when tested by transfection or microinjection in various cell lines. However, the S-ONs with the highest *in vitro* binding affinity are not always the most potent antisense inhibitors. Previous results comparing the antisense activity of thiazole-substituted S-ONs to C5-propynyl-modified S-ONs demonstrated that, although the thiazole-modified ON showed higher affinity for RNA than the C5-propynyl S-ON, the thiazole-

substituted S-ON was a much poorer antisense inhibitor (13). Similarly, the C5-propynyl $p27^{kip1}$ S-ON demonstrated a higher relative affinity for the same target RNA relative to a single substituted G-clamp $p27^{kip1}$ S-ON, yet when transfected into CV-1 cells, the G-clamp S-ON was a more potent antisense inhibitor, as shown in Fig. 3. One possible explanation for the enhanced potency of G-clamp S-ONs is their ability to activate RNase H cleavage. Despite the bulkiness of the G-clamp heterocycle, the G-clamp S-ON/RNA heteroduplex was a 3-fold better substrate for RNase H cleavage relative to the C5-propynyl S-ON/RNA duplex (Table 2). Fine mapping of the RNase H cleavage site of the G-clamp S-ON/RNA hybrid indicated that the cleavage sites adjacent to the G-clamp were unaffected by the aminoethoxy tethering arm in the major groove (data not shown). These results highlight the unique ability of the G-clamp S-ON to hybridize in a selective fashion to its RNA target and to activate RNase H-mediated cleavage of the RNA, resulting in potent antisense-specific gene inhibition.

The *in vitro* binding properties and RNase H activity of the G-clamp S-ON may not be sufficient to explain the enhanced antisense potency observed. S-ON/RNA helix dissociation is known to occur at a much faster rate intracellularly relative to *in vitro* conditions (12). The dissociation process intracellularly is likely mediated by numerous proteins with helicase activity. The G-clamp modification could result in substantial stabilization of the S-ON/RNA duplex intracellularly by rendering the helix a poor substrate for such helicases. This hypothesis awaits further testing.

All first-generation, conventional S-ONs that have entered phase I safety studies have demonstrated safety profiles that have allowed their continued clinical development (26–29). The continued development of the G-clamp modification in antisense-based therapeutics also depends on the demonstration of acceptable safety and pharmacokinetic profiles in preclinical models. ON modifications can dramatically alter the pharmacokinetics of ONs *in vivo* (30). *In vivo* analysis of 2′-*O*-alkyl-modified S-ONs indicated faster plasma elimination and more rapid excretion compared with unmodifed S-Ons (31), and C5-propynyl-modified S-ONs have demonstrated *in vivo* liver toxicities that have precluded their development as human therapeutics (W.M.F. and R.W.W., unpublished results). However, preliminary *in vivo* data suggests that a single G-clamp modification in a 15-mer S-ON does not alter the pharmacokinetic, toxicity, or tissue-distribution properties of the S-ON as compared with a conventional antisense S-ON when dosed as high as 50 mg/kg for 10 days in mice (Steven Davis, personal communication). These preliminary results suggest that G-clamp-modified S-ONs have the appropriate *in vivo* profile to continue their development as a more potent and safer second-generation, antisense-based human therapeutic.

We thank Terry Terhorst for synthesis and purification of the oligonucleotides.

1. Walder, R. Y. & Walder, J. A. (1988) *Proc. Natl. Acad. Sci. USA* **85,** 5011–5015.
2. Zamecnik, P. C. & Stephenson, M. L. (1978) *Proc. Natl. Acad. Sci. USA* **75,** 280–284.
3. Wagner, R. W. (1994) *Nature (London)* **372,** 333–335.
4. Wagner, R. W. (1995) *Antisense Res. Dev.* **5,** 113–114.
5. Matteucci, M. D. & Wagner, R. W. (1996) *Nature (London)* **384,** 20–22.
6. Flanagan, W. M. (1998) *Cancer Metastasis Rev.* **17,** 169–176.
7. Lin, K.-Y. & Matteucci, M. D. (1998) *J. Am. Chem. Soc.* **120,** 8531–8532.
8. Froehler, B. C. (1993) in *Protocols for Oligonucleotides and Analogs: Synthesis and Properties*, ed. Agrawal, S. (Humana, Totowa, NJ), pp. 63–80.
9. Froehler, B. C., Wadwani, S., Terhorst, T. J. & Gerrard, S. R. (1992) *Tetrahedron Lett.* **33,** 5307–5310.
10. Lin, K.-Y., Jones, R. J. & Matteucci, M. (1995) *J. Am. Chem. Soc.* **117,** 3873–3874.
11. Monia, B. P., Johnston, J. F., Greiger, T., Muller, M. & Fabbro, D. (1996) *Nat. Med.* **2,** 668–675.
12. Moulds, C., Lewis, J. G., Froehler, B. C., Grant, D., Huang, T., Milligan, J. F., Matteucci, M. D. & Wagner, R. W. (1995) *Biochemistry* **34,** 5044–5053.
13. Gutierrez, A. J., Matteucci, M. D., Grant, D., Matsumura, S., Wagner, R. W. & Froehler, B. C. (1997) *Biochemistry* **36,** 743–748.
14. Fisher, T. L., Terhorst, T., Cao, X. & Wagner, R. W. (1993) *Nucleic Acids Res.* **21,** 3857–3865.
15. Wagner, R. W., Matteucci, M. D., Lewis, J. G., Gutierrez, A. J., Moulds, C. & Froehler, B. C. (1993) *Science* **260,** 1510–1513.
16. Flanagan, W. M. & Wagner, R. W. (1997) *Mol. Cell. Biochem.* **172,** 213–225.
17. Flanagan, W. M. (1999) in *Manual of Antisense Methodology*, eds. Endres, S. & Hartmann, G. (Kluwer, Boston), in press.
18. Lewis, J. G., Lin, K. Y., Kothavale, A., Flanagan, W. M., Matteucci, M. D., DePrince, R. B., Mook, R. A., Hendren, R. W. & Wagner, R. W. (1996) *Proc. Natl. Acad. Sci. USA* **93,** 3176–3181.
19. Coats, S., Flanagan, W. M., Nourse, J. & Roberts, J. M. (1996) *Science* **272,** 877–880.
20. Flanagan, W. M., Kothavale, A. & Wagner, R. W. (1996) *Nucleic Acids Res.* **24,** 2936–2941.
21. Flanagan, W. M., Su, L. L. & Wagner, R. W. (1996) *Nat. Biotechnol.* **14,** 1139–1145.
22. St. Croix, B., Floerenes, V. A., Rak, J., Flanagan, W. M. & Kerbel, R. S. (1996) *Nat. Med.* **2,** 1204–1210.
23. Monia, B. P. (1997) *Anticancer Drug Des.* **12,** 327–341.
24. Monia, B. P., Sasmor, H., Johnston, J. F., Freier, S. M., Lesnk, E. A., Muller, M., Altmann, K.-H., Moser, H. & Fabbro, D. (1996) *Proc. Natl. Acad. Sci. USA* **93,** 15481–15485.
25. Monia, B. P., Johnston, J. F., Ecker, D. J., Zounes, M. A., Lima, W. F. & Freier, S. M. (1992) *J. Biol. Chem.* **267,** 19954–19962.
26. Srinivasan, S. K. & Iversen, P. (1995) *J. Clin. Lab. Anal.* **9,** 129–137.
27. Geary, R. S., Leeds, J. M., Henry, S. P., Monteith, D. K. & Levin, A. A. (1997) *Anticancer Drug Des.* **12,** 383–393.
28. Henry, S. P., Montieth, D. & Levin, A. A. (1997) *Anticancer Drug Des.* **12,** 395–407.
29. Henry, S. P., Monteith, D., Bennett, F. & Levin, A. A. (1997) *Anticancer Drug Des.* **12,** 409–420.
30. Delong, R. K., Nolting, A., Fisher, M., Chen, Q., Wickstrom, E., Kligshteyn, M., Demirdji, S., Caruthers, M. & Juliano, R. L. (1997) *Antisense Nucleic Acid Drug Dev.* **7,** 71–77.
31. Altmann, K. H., Dean, N. M., Fabbro, D., Freier, S. M., Geiger, T., Haner, R., Husken, D., Martin, P., Monia, B. P., Muller, M., *et al.* (1996) *Chimia* **50,** 168–176.